

THE STABILITY OF THIN-WALLED SINGLE AND MULTI-CELL CFRP COMPOSITE TUBES IN TORSION

J Loughlan ^{a,b} and N B Yidris ^c

^a AAE, Loughborough University, Loughborough, Leicestershire, LE11 3TU, UK
email: j.loughlan@lboro.ac.uk

^b SATM, Cranfield University, Cranfield, Bedfordshire, MK43 0AL, UK
email: joe.loughlan@cranfield.ac.uk

^c Department of Aerospace Engineering, University Putra Malaysia, Selangor, Malaysia
email: nyidris@upm.edu.my

Keywords: CFRP composite tubes; Single and multi-cell tubes; Torsional stability; Local shear buckling; Distortional buckling; Finite strip method; Laminated construction; Finite element simulation; Multi-cell torsion theory.

Abstract. *The buckling performance of thin-walled single and multi-cell CFRP composite tubes in uniform torsion is examined in this paper using both the finite strip and finite element methods of analysis. Due consideration is given in the paper to the influence on performance of flexural anisotropy or the bend-twist coupling characteristics of the composite material. The paper highlights the importance of realising the significance of the applied torque direction on buckling performance. Markedly different stability levels are shown to be in existence for the clockwise and anticlockwise torsional loading cases of the thin-walled multi-cell CFRP composite tubes. This situation is, of course, not realised in isotropic metal construction or in specially orthotropic CFRP composite construction since such material systems are devoid of the effects of material flexural anisotropy and thus the significance of the applied torque direction in this case is no longer appropriate.*

1. INTRODUCTION

The torsional equilibrium of thin-walled polymer composite sections when subjected to free or uniform torsion is achieved through quite different mechanisms for open and closed section profiles. In the case of open sections, channels, top-hats, etc., the applied torque is reacted at any cross-section along the length of the member by the St Venant shear stresses which act in the plane of the cross-section through the thickness of the section walls. These shear stresses vary linearly through the wall thickness and are zero at the mid-plane and maximum at the wall surfaces. In this case the equilibrating stress system is of a non-destabilizing nature and thus increasing the torque simply leads to ultimate conditions devoid of buckling and resulting in material failure due to yielding in metal sections or due to fibre breakage, matrix cracking, or perhaps, ply delamination in polymer composite sections.

For closed section profiles, hollow cylinders, box tubes, multi-cell systems, etc., the applied torque is reacted by the appropriate Bredt-Batho shear flow system acting in the plane of the cross-section and whereby the shear stresses are uniformly constant through the wall thickness. In this case the equilibrating mid-plane stress system in the section walls is destabilizing in nature and thus increasing the torque can lead to buckling in the earlier stages of loading prior to ultimate conditions. Local shear buckling in the closed section walls can occur under uniform torque as well as torsional buckling and coupled local-shear/torsional distortional type buckling. To the author's knowledge, with the exception of composite cylindrical shells and drive shafts, there is a dearth of information in the open literature relating to the buckling of polymer composite closed cell sections subjected to uniform torsion, especially for multi-cell

systems and for laminate materials which possess bend-twist coupling. There is a clear lack of detailed information and consequently there is the need and scope for further work to be carried out in this area of research in order to expand our knowledge and understanding of the behaviour of these closed section polymer composite structural members in torsion.

Meyer-Piening et al [1] give a detailed outline of work carried out in the early to late nineties with regard to experiments and computations relating to the buckling of CFRP composite cylinders under combined axial and torsional loading. Computations included shallow shell theory, deep shell theory and finite element simulation and the data obtained from this work was considered to be a useful benchmark reference. The shear buckling of CFRP composite hollow cylindrical drive shafts under torsion have been studied by Shokrieh et al [2]. The torsional buckling loads of the hollow shafts for different ply lay-up configurations have been determined through finite element simulation and a good comparison with the results from independent experimental work is indicated.

Cherniaev and Komarov [3] have considered the problem of a carbon-epoxy drive shaft design by means of a multistep optimisation process. The drive shaft considered is part of a helicopter transmission system and is essentially a thin-walled tube with 100 mm internal diameter and of length 1400 mm. Buckling was shown to be the active constraint in this work. Hu et al [4] have highlighted the different failure mechanisms of CFRP composite circular hollow drive shafts under clockwise and counter-clockwise torque. This work precluded buckling and used the Tsai-Wu failure criterion to predict torsional capacity.

Goncalves and Camotim [5] have used Generalised Beam Theory and shell finite element modelling to obtain results for the local shear buckling modes of regular polygonal tube members under uniform torsion. Isotropic material was considered and close agreement between these two analysis procedures was registered. Omidvari and Hematiyan [6] have developed some closed form design formulae for the buckling response of hollow rectangular tubes under uniform and non-uniform torsion. This work is for isotropic materials and can predict the local shear mode for thin-walled tubes and the distortional mode for tubes with thicker walls.

Rendall et al [7] have used the generalised finite strip method, cFSM, to determine the buckling behaviour of long polygonal tubes in uniform torsion. Signature curves of long polygonal tubes with triangular through octagonal cross-sections in uniform torsion are detailed in this work with material properties being assumed to be isotropic. Kołakowski and Jankowski [8] have studied the stability of thin-walled square tubes with intermediate stiffeners and also square tubes and regular octagon tubes without stiffeners under torsion. Their finite element work considered constrained torsion whilst the work of reference [7] in their comparative studies relates to the case of free uniform torsion.

As mentioned previously, isotropic tubes under uniform torsion [5-8] yield the same critical buckling torques when subjected to clockwise or anti-clockwise torque. The same is not true for CFRP laminated composite tubes as a result of the flexural anisotropy or bend-twist coupling characteristics of the laminated composite material. This has been shown with regard to torsional capacity [4] where the composite tube design is governed by material failure and quite different failure modes are in evidence for the cases of +ve and -ve torque.

The buckling of CFRP thin composite plates in shear and thin-walled square composite tubes in free torsion have been studied by Loughlan [9] whilst the stability of perforated CFRP composite plates in shear have been considered by Yidris et al [10]. In these works [9,10] due consideration has been given to the effects of bend-twist coupling and to the applied shear/torque direction on buckling performance. Significantly different stability levels have been shown to exist between the two directions and thus careful consideration is needed in design.

In this paper the work of reference [9] is extended to deal with multi-cell CFRP composite

tubes with flat walls and subjected to uniform free torsion. The results presented have been obtained using a finite strip formulation which has been developed for layered composite materials and which is able to account for the various different forms of laminate material mechanical couplings. Extensive use has also been made of the Abaqus FE simulation procedures and this two pronged approach has provided the authors with a deep understanding of the stability mechanics of the multi-cell systems as well as giving a high degree of confidence in the findings from this work. Results are presented for one, two and three cell tubes with flat walls and the finite strip formulation and its applications have been validated against the Abaqus FE numerical simulation work in which case virtually identical results are achieved. The finite strip formulation is a new multi-term configuration which utilises six longitudinal harmonics in the buckling perturbation deflection series of the strip and thus it is capable of a high degree of stiffness flexibility and, as a result, is able to deal effectively with complex structural configurations involving several different buckling modes including those of a coupled nature.

2. PRE-BUCKLED SHEAR FLOWS USING MULTI-CELL TORSION THEORY

Multi-cell tubes subjected to uniform torsion develop a unique set of shear flows q_i in the individual cells which are easily and readily determined through application of Bredt-Batho multi-cell torsion theory. Figure 1 shows the pre-buckled shear flows for a CFRP composite 3-cell tube with 50x50 mm cells. The walls are 1 mm thick and have a lay-up configuration of $[(\pm 45^\circ)_2]_s$, i.e. 8 plies with a ply thickness of 0.125 mm. The tube is manufactured from high-strength carbon-epoxy pre-impregnated ply sheets with the ply material properties; $E_1 = 140\text{kN/mm}^2$, $E_2 = 10\text{kN/mm}^2$, $G_{12} = 5\text{kN/mm}^2$, and $\nu_{12} = 0.3$. The pre-buckled shear flows (N/mm) shown in Figure 1 are according to the applied uniform torque $T = 1 \times 10^6$ Nmm. In the paper the pre-buckled shear flows in the multi-cell systems are determined using the bredt-batho procedures and these are then used as the in-plane shear loading in the tube walls in the new multi-term finite strip formulation to obtain the critical buckling torques.

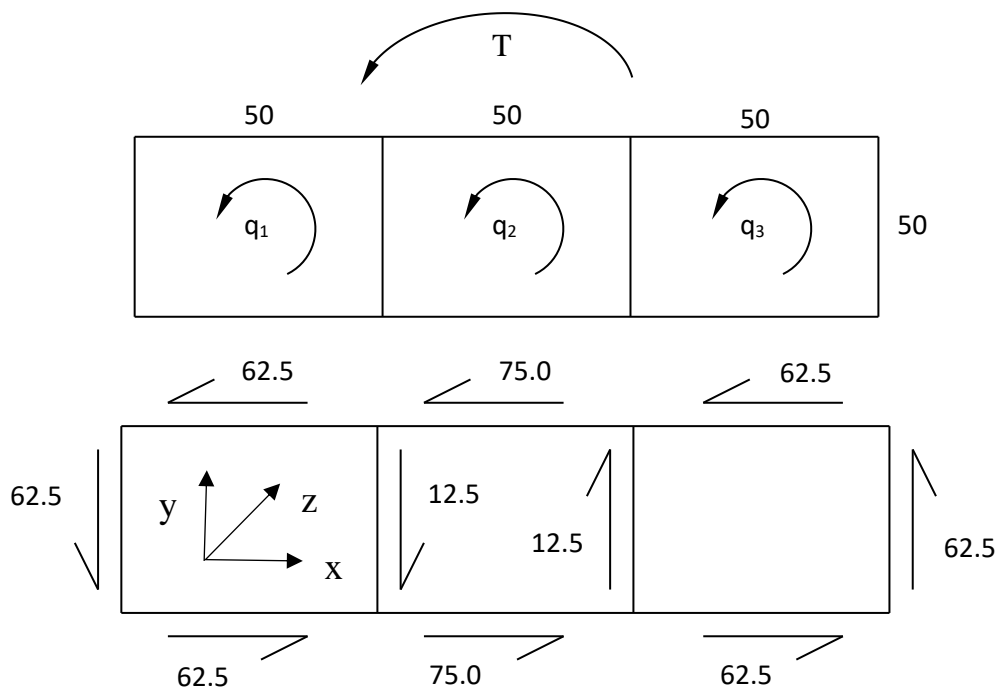


Figure 1: Shear flows (N/mm) in 3-cell tube subjected to uniform torque $T = 1 \times 10^6$ Nmm

3. FINITE STRIP FORMULATION AND MODELLING STRATEGY

To determine the buckling behaviour of the CFRP composite multi-cell tubes under uniform torsion a classical basic multi-term finite strip formulation developed for layered composite materials, has been employed. The finite strip formulation employed is essentially an upgraded version of that used in the previous study of reference [9], in that it is now capable of a much higher degree of stiffness flexibility due to its increased multi-term nature and thus it is able to deal more effectively with complex structural configurations involving different buckling modes including those of a coupled nature. The finite strip is simply supported at its ends and the strip perturbation or buckling displacement fields are postulated to vary sinusoidally along the strip length and algebraically across the strip width with any combination of linearly varying bi-axial tension or compression coupled with in-plane shear loading on the strip being able to be accommodated. For the case of the multi-cell tubes in uniform torsion, the loading on the strips will be pure in-plane shear and for the 3-cell tube with 50x50 mm cells the shear loading on the strips will be those detailed in Figure 1 in accordance with a uniform applied torque $T = 1 \times 10^6$ Nmm. Figure 2 shows a schematic of the finite strip discretisation of a composite square box tube $b \times b \times L$ subjected to uniform torque T . The longitudinal strips are connected at their nodal lines such that the compatibility of displacements and slopes are maintained throughout the structural assembly. The strip geometry, coordinate axis system and u, v, w displacements are detailed in Figure: 3.

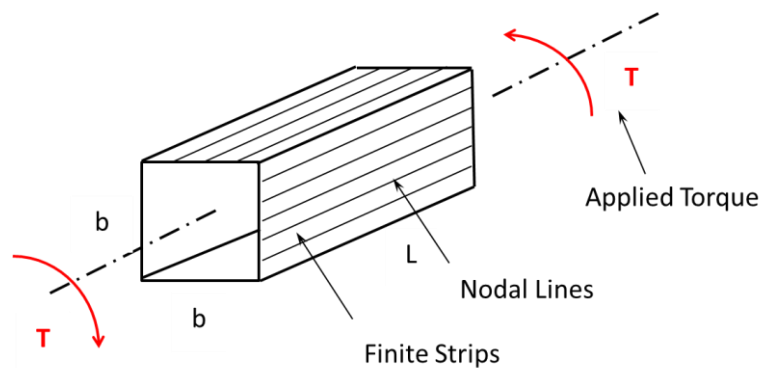


Figure 2: Discretisation of composite box tube subjected to uniform torque.

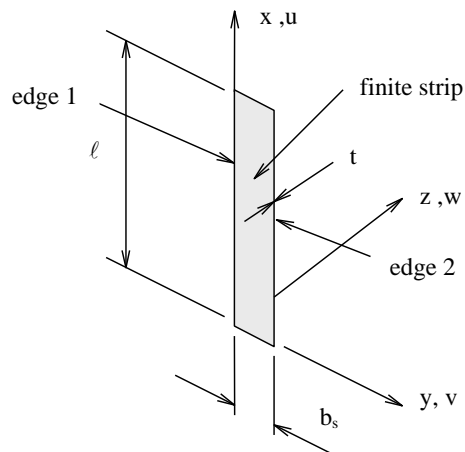


Figure 3: Strip geometry, co-ordinate axes system and displacements.

In reference [9], the number of longitudinal sinusoidal harmonics ‘n’ in the strip perturbation displacement fields is $n = N = 3$. The displacement connection quantities $u_{1n}, v_{1n}, w_{1n}, \theta_{1n}$, on edge 1 and $u_{2n}, v_{2n}, w_{2n}, \theta_{2n}$, on edge 2 of the strip corresponding to the n^{th} harmonic of the buckling deflection series is shown in Figure: 4. In reference [9] the size of the local elastic and geometric stiffnesses $[k]$ and $[k_{\sigma}]$ for an individual finite strip based on $N = 3$ is 24×24 with 12 displacement connection quantities along each edge or nodal line of the strip. The finite strip formulation procedures are outlined in considerable detail in reference [9] including strip assembly to form the global elastic and geometric stiffnesses $[K]$ and $[K_{\sigma}]$ for a given structure as well as the eigenvalue solution procedure for critical stability.

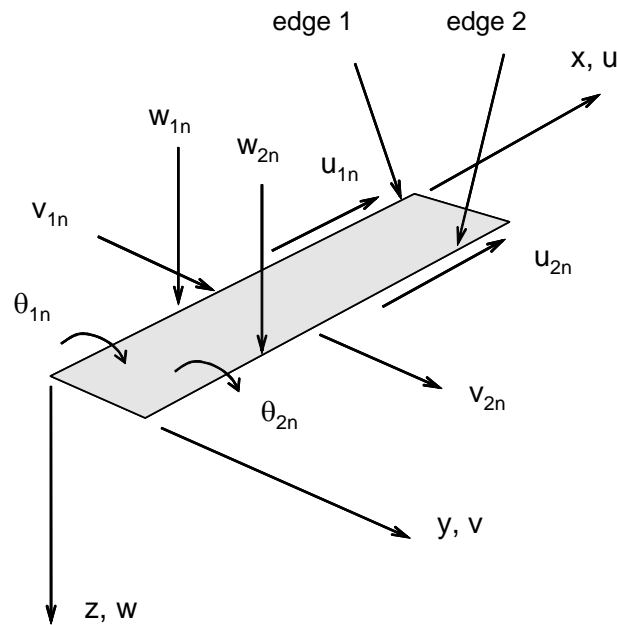


Figure 4: Displacement connection quantities corresponding to the n^{th} harmonic of the buckling deflection series.

In the current work of this paper on multi-cell composite tubes in uniform torsion the new finite strip formulation is based on six longitudinal harmonics and this has been deemed necessary in order to provide a higher degree of strip flexibility in order to facilitate a wider range of application of the finite strip approach. With $N = 6$ the size of the local stiffnesses $[k]$ and $[k_{\sigma}]$ is now 48×48 with 24 displacement connection quantities along each edge or nodal lines of the strip. Figure 5: shows the edge displacement connection quantities for the first six harmonics of the buckling perturbation deflection series of the new formulation.

The six harmonics used in the new finite strip analysis procedures are any six general consecutive harmonics defined by n,m,p,q,r,s and thus we could employ, for example, $n,m,p,q,r,s = 1,2,3,4,5,6$ or $2,3,4,5,6,7$, or $3,4,5,6,7,8$ in the sinusoidal buckling displacement series and thus, in this way, we are able to quite readily pick up the local shear buckling mode in the walls of long composite tubes in torsion with many shear buckles along the tube length simply by choosing the appropriate range for n,m,p,q,r,s . The appropriate range of harmonics can be determined iteratively in the developed finite strip programme which has been written in the FORTRAN programming language and thus the minimum critical torques are realised for the clockwise and anti-clockwise loading cases.

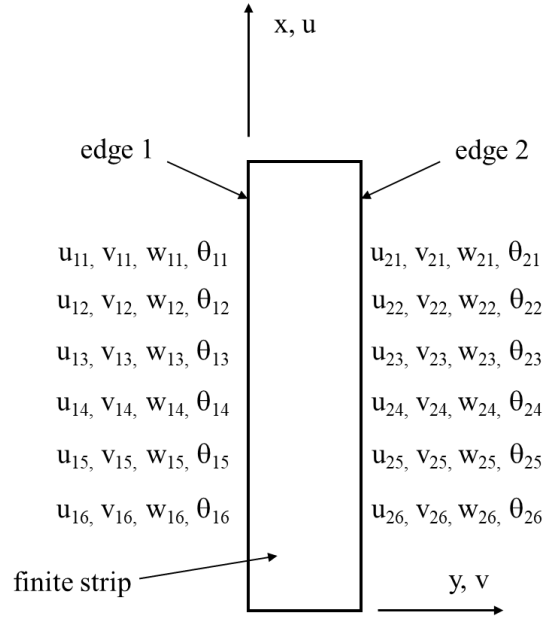


Figure 5: Edge displacement connection quantities for the first six harmonics of the buckling deflection series.

The accuracy of the finite strip solutions depends to a large extent on the number of strips used to model the cross-section buckling perturbations as well as to the number of strip sinusoidal longitudinal harmonics used in order to capture the buckling perturbations along the length of the multi-cell tubes. When modelling the 3-cell tube subjected to uniform torque as detailed in Figure 1:, the number of strips in each flat wall is 8 and thus 80 strips reflects the complete structural assembly with 78 nodal lines and 24 local degrees of freedom per node and thus there are 1872 active degrees of freedom in the assembled constrained structural model.

The size of the finite strip eigen-solution for the 3-cell tube using 80 strips to represent the cross-section is always 1872 active degrees of freedom of the constrained assembled model irrespective of the tube length since the finite strip programme is able to iteratively select the appropriate range for the six consecutive sinusoidal harmonic parameters n, m, p, q, r, s such that the minimum critical torques are determined for the clockwise and counter-clockwise directions. This is in contrast to the modelling procedures in finite element simulation whereby the size of the eigen-solution continues to increase with increase in the 3-cell tube length as more and more elements are required in the model.

4. FINITE ELEMENT SIMULATION PROCEDURES

The finite element simulations of the multi-cell CFRP tube systems have been carried out using the S4R5 shell element of the ABAQUS finite element software. This is a 4-node doubly curved thin shell with reduced integration, hourglass control, and with five degrees of freedom per node, 3-translations and 2-in-plane rotations; there are no rotations about the shell normal of the S4R5 element. Clearly the accuracy of the simulation process depends essentially on a suitably refined finite element model which encompasses both the appropriate loading and support boundary conditions of the actual structural system. Structural models have been set-up using 5 mm elements and also 3 mm elements for extremely refined buckling solutions.

When considering the 3-cell CFRP tube of Figure 1: and using 5 mm elements, this gives 10 elements in each flat wall of the cross-section, i.e. 100 elements to model the cross-section resulting in 98 nodes. Considering a tube length $Z = L = 600$ mm, this represents 120 elements

along the length of the tube giving a total of $98 \times 121 = 11,858$ nodes which represents 59,290 degrees of freedom for the assembled structural model free of constraints. Constraining the model to realise uniform torsion means allowing free warping at each end of the 3-cell tube. With reference to Figure 1: all 98 nodes at $Z = L = 600$ mm are constrained in x and y . In addition the 2 nodes on the vertical axis of symmetry of the cross-section and the 4 nodes on the horizontal axis of symmetry are constrained in z , these 6 nodes being the zero warping locations of the cross-section in uniform torsion. The Torque T is applied at the shear centre of the cross-section at $Z = 0$ using multi-point constraint (MPC) in conjunction with 98 rigid body elements connecting the master node at the section shear centre to the 98 slave nodes around the cross-section profile. This ensures that all 98 nodes at $Z = 0$ are constrained to have the same θ_z rotation and that the cross-section is not distorted and maintains its shape as well as allowing for free warping.

The total number of constraints on the structural model is therefore 300 resulting in the active degrees of freedom of the constrained model being 58,990. This should be compared with the value of 1,872 from the finite strip constrained solution when using 80 strips in the structural model. Here we see that the FE eigen-solution is 31.512 times larger than the FS solution whilst it is shown in the paper that both procedures are giving almost the same results within a few percent. When considering a tube length $Z = L = 1000$ mm, we find that the active degrees of freedom of the FE constrained model is now 98,190 and that the FE eigen-solution is now 52.45 times larger than the FS solution. It has to be noted that the iterative procedures in the finite strip FORTRAN programme ensures that the active degrees of freedom of the constrained finite strip model is indeed 1,872 for all lengths of the 3-cell composite tube.

5. SOME TYPICAL RESULTS AND DISCUSSION

In all of the results presented, the CFRP single and multi-cell tubes are considered to be manufactured from high-strength carbon-epoxy pre-impregnated ply sheets with a ply thickness of 0.125 mm and with the ply material properties; $E_1 = 140\text{kN/mm}^2$, $E_2 = 10\text{kN/mm}^2$, $G_{12} = 5\text{kN/mm}^2$, and $\nu_{12} = 0.3$. Figure 6: shows the buckled modes of a single-cell CFRP tube in free torsion. The tube length $L = 800$ mm and its cross-section is 100×50 mm with $t = 1$ mm wall thickness consisting of 8 plies with the layup configuration of $[(\pm 45^\circ)_2]_s$. The finite strip analysis used 80 strips to model this cross-section, 30 strips in the wide 100 mm flanges and 10 strips in the 50 mm webs whilst the finite element simulation used some 26,700 3mm S4R5 shell elements. Finite strip simulation gives a +ve critical torque of $T_{CR} = 26.3307 \times 10^4$ Nmm corresponding to the Local Shear mode in Figure 6(a) with the ratio of FE/FS = 1.026 i.e. the solutions are within 2.6% of each other. The -ve critical torque is $T_{CR} = 38.7137 \times 10^4$ Nmm from finite strip corresponding to the Torsional-Distortional mode in Figure 6(b) with the ratio of FE/FS = 0.9625 i.e. the solutions are within 3.8%.

It is of note that the ratio $-veT_{CR}/+veT_{CR}$ is 1.4703 i.e. -ve or anticlockwise torque gives a 47% greater stability performance over +ve or clockwise torque due, essentially, to the bend-twist coupling characteristics of the CFRP composite tube walls. Also of some significance is the quite different buckling modes for the two torque directions with predominant Local Shear buckling, Figure 6(a), occurring in the wide flange elements of the tube for the case of +ve torque with clearly defined amplitude modulation of the shear buckles in evidence indicating heavier buckles over the mid-length of the tube and with diminishing amplitudes towards the loaded ends. In the case of -ve torque the mode of buckling, Figure 6(b), is of a Global Torsional-Distortional type, there is clear evidence of twisting along the tube length as well as predominant local shear effects in the wide flange elements of the tube.

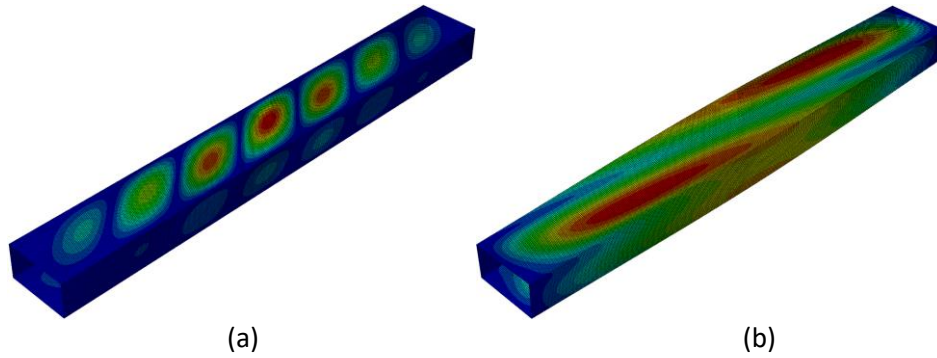


Figure 6: Buckled modes of single-cell CFRP tube, $t = 1$ mm, $L = 800$ mm.
 (a) +ve or Clockwise Torque, Local Shear mode.
 (b) -ve or Anticlockwise Torque, Torsional-Distortional mode.

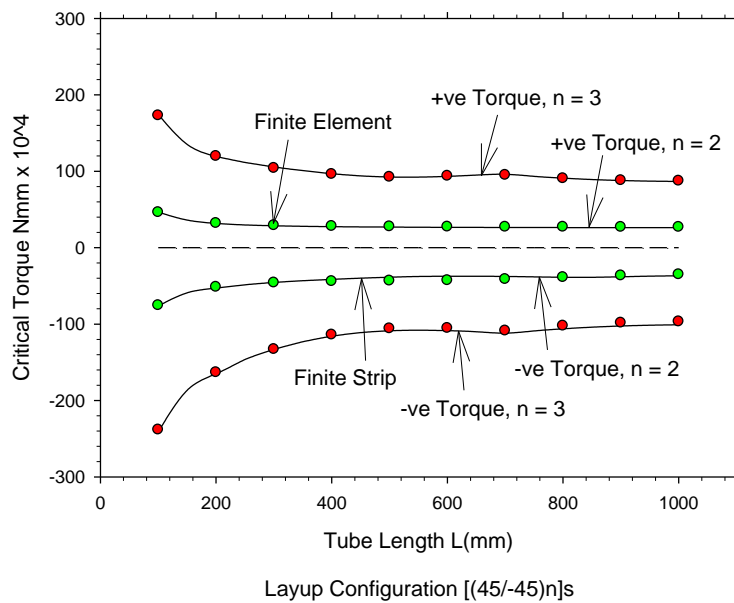


Figure 7: Critical buckling torques for the 100x50 mm CFRP composite tubes.

Figure 7: shows the comparisons between the finite strip and finite element simulations for the critical buckling torques of the 100x50 mm CFRP composite tubes in free torsion according to the tube length range of 100-1000 mm. The lay-up configuration of the tube walls is $[(\pm 45^\circ)_n]_s$ where $n = 2$ gives a wall thickness of $t = 1$ mm and $n = 3$ gives a wall thickness of $t = 1.5$ mm. The full lined curves in Figure 7: are those from finite strip simulation whilst the markers are those from finite element analysis. Remarkably good agreement is seen to exist between the two procedures. Increasing the wall thickness to $t = 1.5$ mm is found to effectively eliminate the occurrence of the local shear mode under +ve uniform torque loading for tube lengths greater than about 300 mm and thus, in this case, the buckled modes for +ve and -ve torque are both of the Torsional-Distortional format.

This is detailed in Figure 8: for the tube length $L = 800$ mm and for the cross-section 100x50 mm with a wall thickness $t = 1.5$ mm consisting of 12 plies with the layup configuration of $[(\pm 45^\circ)_3]_s$. Finite strip simulation gives a +ve critical torque of $T_{CR} = 91.0119 \times 10^4$ Nmm corresponding to the Torsional-Distortional mode in Figure 8(a) with the ratio of FE/FS = 0.9956 i.e. the solutions are almost identical. The -ve critical torque is $T_{CR} = 106.9615 \times 10^4$ Nmm from finite strip corresponding to the Torsional-Distortional mode in Figure 8(b) with

the ratio of $FE/FS = 0.9639$ i.e. the solutions are within 3.6%. For the 1.5 mm thick tube anticlockwise torque is found to give a 17.5% greater stability performance over clockwise torque.

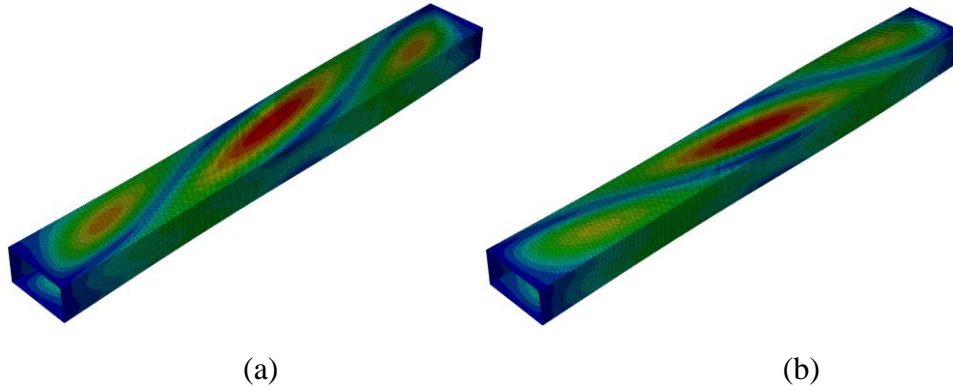


Figure 8: Buckled modes of single-cell CFRP tube, $t = 1.5$ mm, $L = 800$ mm.
 (a) +ve or Clockwise Torque, Torsional-Distortional mode.
 (b) -ve or Anticlockwise Torque, Torsional-Distortional mode.

Figure 9: shows the buckled modes of a 2-cell CFRP tube in free torsion. The tube length $L = 600$ mm and its cross-section consists of two 50×50 mm cells enabling three webs with the overall cross-section being 100×50 mm. The wall thickness $t = 1$ mm and consists of 8 plies with the layup configuration of $[(\pm 45^\circ)_2]_s$. Under uniform torsion the middle web of the 2-cell tube doesn't warp and it doesn't carry any shear flow and thus the torsional shear flow is carried solely by the peripheral flat walls of the 2-cell tube. Adding the middle web to the single-cell tube doesn't alter its torsional stiffness but it does provide significant local support to its wide flange elements and thus the torsional stability of the 2-cell tube is found to be a substantial improvement on its single-cell equivalent.

Finite strip simulation gives a +ve critical torque of $T_{CR} = 87.4117 \times 10^4$ Nmm corresponding to the Local Shear mode in Figure 9(a) with the ratio of $FE/FS = 1.00582$. The -ve critical torque is $T_{CR} = 145.644 \times 10^4$ Nmm from finite strip corresponding to the Local Shear mode in Figure 9(b) with the ratio of $FE/FS = 1.00458$. For the 1.0 mm thick 2-cell CFRP tube anticlockwise torque is found to give a 66.6% greater stability performance over clockwise torque.

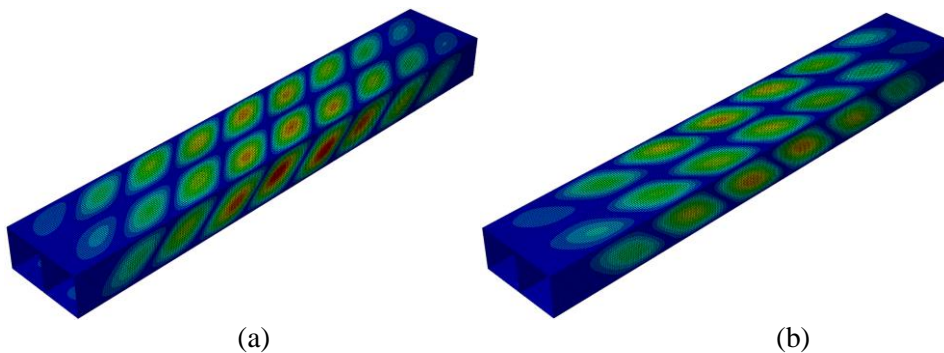


Figure 9: Buckled modes of 2-cell CFRP tube, $t = 1$ mm, $L = 600$ mm.
 (a) +ve or Clockwise Torque, Local Shear mode.
 (b) -ve or Anticlockwise Torque, Local Shear mode.

Figure 10: shows the local shear stability of 2-cell CFRP composite tubes subjected to free uniform torsional loading. Nondimensional critical shear flow N_{xy} is shown plotted against the tube length L over the length range 100-1000 mm. Again, the cross-section of the tubes consists of two 50×50 mm cells enabling three webs with the overall cross-section being 100×50 mm. Two wall thickness have been considered $t = 0.5$ mm and $t = 1$ mm consisting of 4 plies and 8

plies respectively with $n = 1$ and 2 respectively corresponding to the layup configuration of $[(\pm 45^\circ)_n]_s$.

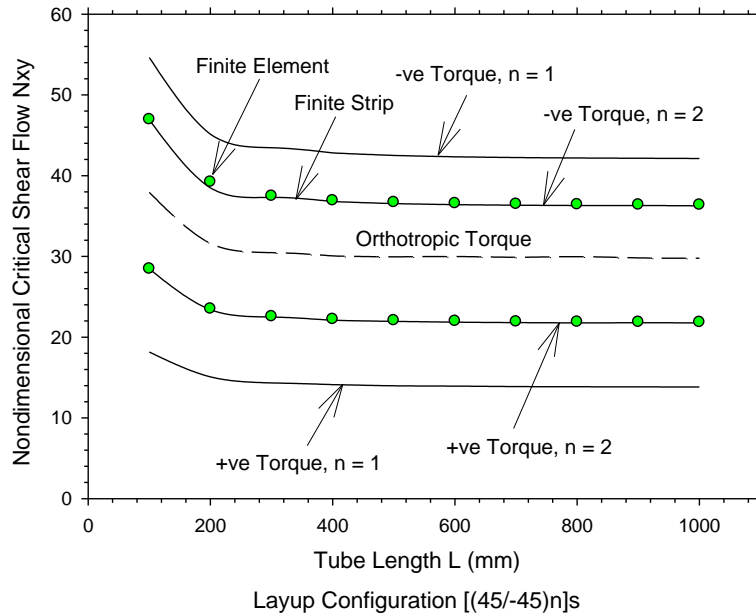


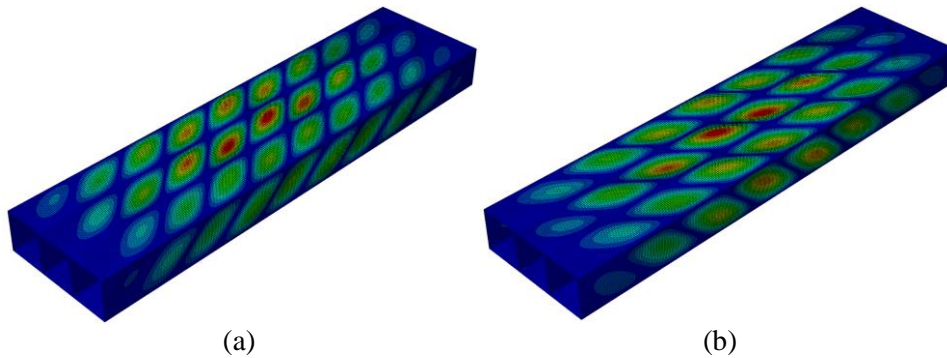
Figure 10: The local shear stability of 2-cell CFRP composite tubes in torsion.

Due to the double symmetry of the cross-section the reactive shear flow to the applied torque is carried solely by the peripheral boundary walls of the tubes since the mid-web does not warp and does not carry any shear flow. In this case the nondimensional critical shear flow N_{xy} is given in terms of the applied critical torque T_{CR} as; $N_{xy} = T_{CR}/4E_2t^3$. The full lined curves in Figure 10: are those from finite strip simulation and the markers are from finite element analysis for the wall thickness $t = 1$ mm whereby the ratio FE/FS is found to be remarkably close to unity across the complete length range, i.e. within 1%.

The broken lined curve is the FS orthotropic solution which precludes the influence of the flexural anisotropy of the CFRP composite material. In this case the clockwise and anticlockwise torque directions yield the same level of critical shear flow and as such the orthotropic solution should not be used in design. This approach can be conservative or unconservative depending on the applied torque direction when used to predict the critical torque levels of thin-walled CFRP systems which possess flexural anisotropy.

As an example, for the 0.5 mm thick 2-cell CFRP tube with $L = 600$ mm, finite strip simulation gives a +ve critical torque of $T_{CR} = 6.96605 \times 10^4$ Nmm and a -ve critical torque of $T_{CR} = 21.1685 \times 10^4$ Nmm whilst the orthotropic torque is $T_{CR} = 15.0662 \times 10^4$ Nmm. This corresponds to the nondimensional shear flows in Figure 10 of $N_{xy} = 13.9321, 42.337$ and 30.1323 respectively for $L = 600$ mm. In this case the stability performance level of anticlockwise torque is found to be more than 3 times that of clockwise torque. It is also of note that the orthotropic torque overestimates the +ve torque by 116.28% and underestimates the -ve torque by 28.83%.

Figure 11: shows the buckled modes of a 3-cell CFRP tube in free torsion. The tube length $L = 600$ mm and its cross-section consists of three 50×50 mm cells enabling four webs with the overall cross-section being 150×50 mm. The wall thickness $t = 1$ mm and consists of 8 plies with the layup configuration of $[(\pm 45^\circ)_2]_s$. Under uniform torsion there are six zero warping locations on the 3-cell cross-section, four on the horizontal axis of symmetry in the webs and two on the vertical axis of symmetry in the flanges of the middle cell.



(a) (b)
 Figure 11: Buckled modes of 3-cell CFRP tube, $t = 1$ mm, $L = 600$ mm.
 (a) +ve or Clockwise Torque, Local Shear mode.
 (b) -ve or Anticlockwise Torque, Local Shear mode.

Finite strip simulation gives a +ve critical torque of $T_{CR} = 137.3973 \times 10^4$ Nmm corresponding to the Local Shear mode in Figure 11(a) with the ratio of FE/FS = 1.01066. The -ve critical torque is $T_{CR} = 223.8533 \times 10^4$ Nmm from finite strip corresponding to the Local Shear mode in Figure 11(b) with the ratio of FE/FS = 1.009335. For the 1.0 mm thick 3-cell CFRP tube anticlockwise torque is found to give a 62.9% greater stability performance over clockwise torque.

Figure 12: shows the local shear stability of 3-cell CFRP composite tubes subjected to free uniform torsional loading. Nondimensional critical shear flow N_{xy} is shown plotted against the tube length L over the length range 100-1000 mm. Again, the cross-section of the tubes consists of three 50x50 mm cells enabling four webs with the overall cross-section being 150x50 mm. Two wall thickness have been considered $t = 0.5$ mm and $t = 1$ mm consisting of 4 plies and 8 plies respectively with $n = 1$ and 2 respectively corresponding to the layup

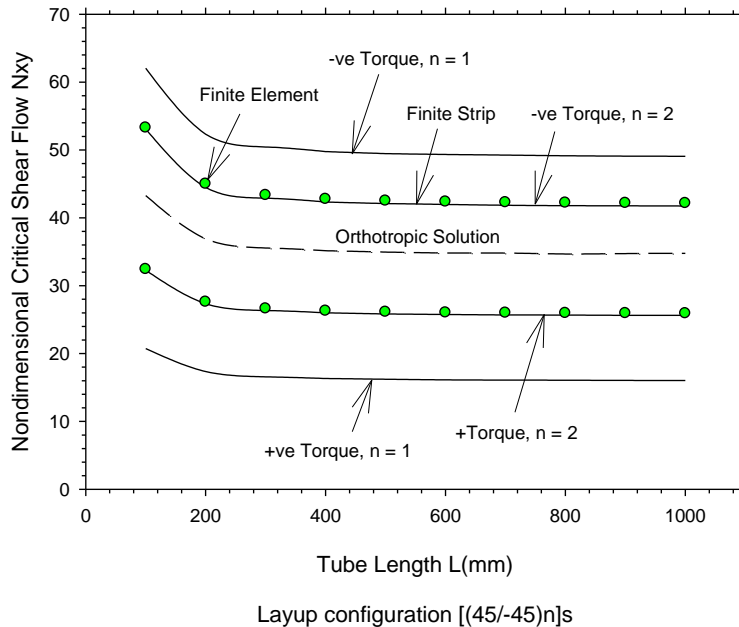


Figure 12: The local shear stability of 3-cell CFRP composite tubes in torsion.

configuration of $[(\pm 45^\circ)_n]_s$. The reactive shear flow system in the walls of the 1 mm thick 3-cell tube has been shown previously in Figure 1 corresponding to the applied uniform torque level of $T = 1 \times 10^6$ Nmm. The nondimensional critical shear flow system N_{xy} shown in Figure 12 is then given in terms of the applied critical torque T_{CR} as; $N_{xy} = 3T_{CR}/16E_2t^3$.

For the 0.5 mm thick 3-cell CFRP tube with $L = 600$ mm, finite strip simulation gives a +ve critical torque of $T_{CR} = 10.7517 \times 10^4$ Nmm and a -ve critical torque of $T_{CR} = 32.8896 \times 10^4$ Nmm whilst the orthotropic torque is $T_{CR} = 23.2170 \times 10^4$ Nmm. This corresponds to the nondimensional shear flows in Figure 12 of $N_{xy} = 16.1276, 49.3344$ and 34.8255 respectively for $L = 600$ mm. In this case the stability performance level of anticlockwise torque is found once again to be more than 3 times that of the clockwise torque. It is also of note that the orthotropic torque overestimates the +ve torque by 115.94% and underestimates the -ve torque by 29.41%. For the 1 mm thick 3-cell tubes it is of note in Figure 12: that the ratio FE/FS is once again remarkably close to unity across the complete length range, i.e. within 0.4-1.13%.

6. CONCLUDING REMARKS

The stability of thin-walled single and multi-cell CFRP composite tubes in uniform torsion has been studied in this paper using Finite Strip and Finite Element simulation. Local shear buckling in the tube walls as well as coupled local shear and torsional buckling of the tubes have been predicted. The influence of flexural anisotropy has been shown to be of significance with quite different critical torque levels being in evidence for the clockwise and anticlockwise torsional loading cases. For the case of the local shear buckling mode it has been shown that the ratio of $-veT_{CR}/+veT_{CR} > 3$ for $t = 0.5$ mm and > 1.6 for $t = 1.0$ mm. For isotropic construction or specially orthotropic CFRP construction the ratio of -ve/+ve torque is equal to unity and thus the applied torque direction in this case is no longer of significance. It is clear from the work presented that the orthotropic approach should not be used in design since this can be both conservative and unconservative depending on the torque direction.

REFERENCES

- [1] Meyer-Piening H.R. Farshad M. Geier B. and Zimmermann R. "Buckling loads of CFRP composite cylinders under combined axial and torsion loading - experiments and computations", *Composite Structures*, 53 (2001) 427-435.
- [2] Shokrieh M.M. Hasani A. and Lessard L.B. "Shear buckling of a composite drive shaft under torsion", *Composite Structures*, 64 (2004) 63-69.
- [3] Cherniaev A. and Komarov V. "Multistep optimization of composite drive shaft subject to strength, buckling, vibration and manufacturing constraints", *Applied Composite Materials*, 22 (2015) 475-487.
- [4] Hu Y. Yang M. Zhang J. Song C. and Zhang W. "Research on torsional capacity of composite drive shaft under clockwise and counter-clockwise torque", *Advances in Mechanical Engineering*, (2015) 1-7.
- [5] Gonçalves R. and Camotim D. "Buckling behaviour of thin-walled regular polygonal tubes subjected to bending or torsion", *Thin-Walled Structures*, 73 (2013) 185-197.
- [6] Omidvari A. and Hematiyan M.R. "Approximate closed-form formulae for buckling analysis of rectangular tubes under torsion", *International Journal of Engineering*, vol. 28 No. 8 (August 2015) 1226-1232.
- [7] Rendall M.A. Hancock G.J. and Rasmussen K.J.R. "Modal buckling behaviour of long polygonal tubes in uniform torsion using the generalised cFSM", *Thin-Walled Structures*, 128 (2018) 141-151.
- [8] Kołakowski Z. and Jankowski J. "Stability of thin-walled square tubes with intermediate stiffeners under torsion", *Journal of Theoretical and Applied Mechanics*, 57 No. 3 (2019) 655-663.
- [9] Loughlan J. "The buckling of CFRP composite plates in compression and shear and thin-walled composite tubes in torsion – The effects of bend-twist coupling and the applied shear direction on buckling performance", *Thin-Walled Structures*, 138 (2019) 392-403.
- [10] Yidris N. Osman I.S. and Gires E. "Influence of shear direction on the buckling of CFRP composite perforated plate", *Forces in Mechanics*, 9 (2022) 100146.